Measurement of the lithium $10p$ fine structure interval and absolute energy

Paul Oxley and Patrick Collins

Physics Department, College of the Holy Cross, 1 College Street, Worcester, Massachusetts, USA

We report a measurement of the fine structure interval of the ^{7}Li $10p$ atomic state with a precision significantly better than previous measurements of fine structure intervals of Rydberg ^{7}Li p states. Our result of 74.97 (74) MHz provides an experimental value for the only $n = 10$ fine structure interval which is yet to be calculated. We also report a measurement of the absolute energy of the $10p$ state and its quantum defect, which are, respectively, 42379.498(23) cm^{-1} and 0.04694 (10). These results are in good agreement with recent calculations.

I. INTRODUCTION

In the past two decades, there has been considerable progress in determining theoretical and experimental values for fine structure intervals [1–6] and energy levels [7–10] of Rydberg states of ^{7}Li. The most precise fine structure measurements to date are of the high-angular-momentum states $10g$, $10h$, and $10i$ [5] and $9f$ and $9g$ [6], which were measured to a few parts per million. The most precise Rydberg nd-state intervals have been measured for $n = 8$–10 with a precision of between 1.1% and 3.5% [3]. Surprisingly, only one previous experiment has determined the fine structure intervals of Rydberg ^{7}Li p states [4]. This experiment reported the $18p$, $21p$, $23p$, $24p$, $25p$, $29p$, $30p$, and $35p$ intervals with an experimental precision of between 5.3% and 19%. Theoretical fine structure calculations for the $10d$ and $10f$ states [1] and the $n = 10$, $4 \leqslant l \leqslant 9$ states [2] have been made. For the $n = 10$ states of ^{7}Li, therefore, the fine structure intervals for every state *except* the p state have been calculated. Here we report a measurement of this interval with a precision five times greater than the previous p-state measurements [4].

We also report a precise measurement of the absolute energy of the $10p$ atomic state. Precise measurements of np energy levels have been made for $n \leqslant 6$ [10] and $n \geqslant 15$ [9]. The energies of np states with $7 \leqslant n \leqslant 14$ have been measured [11,12] but with relatively low precision. Our measurement of the $10p$ energy is more precise by a factor of fifteen than the corresponding results in Refs. [11,12]. Our result for the $10p$ energy is used to test the accuracy of recent calculations for the energies of the ^{7}Li np series [7] and could be used as input for high-accuracy measurements of electric fields using Rydberg atoms [13].

II. EXPERIMENT

The experimental apparatus used for our measurement is shown in Fig. 1. A custom vacuum chamber (not shown) houses a stainless steel oven in which lithium is heated to 470°C. Lithium diffusing from the oven is collimated by a 4-mm aperture situated 190 mm from the oven exit and then intersects a total of four overlapping laser beams. At the intersection region the lithium beam has a diameter of 4.5 mm and the atomic density is estimated to be 5×10^7 atoms/cm^3. The four lasers, which are all grating stabilized diode lasers, excite ^{7}Li to the $10p$ atomic state. The laser frequencies are controlled

by applying a voltage to a piezoelectric transducer (PZT) mounted on the diffraction grating, and their wavelengths are monitored by a wavemeter (Advantest TQ8325).

Lasers L1a and L1b excite ^{7}Li to the $2P_{3/2}$ state from both ground-state hyperfine levels (inset Fig. 1). Laser L2 stimulates the $2P_{3/2} \rightarrow 3S_{1/2}$, $F = 2$ transition, and L3 subsequently excites the atoms to the $10p$ state. Laser L3 can be retroreflected back through the lithium beam to ensure that Doppler shifts are reduced to a negligible level for our measurements. Lasers L1a, L1b, and L2 saturate their transitions but L3 does not.

The optical frequencies of L1a, L1b, and L2 are locked to their transitions by phase-sensitively detecting the $2P_{3/2} \rightarrow 2S_{1/2}$ and $3S_{1/2} \rightarrow 2P_{3/2}$ fluorescence. With L1a, L1b, and L2 locked, successful excitation to the $10p$ states by L3 is confirmed by observing the $10p \rightarrow 2S_{1/2}$ fluorescence. This fluorescence at 236 nm is well separated from all other fluorescence wavelengths and can be detected with high efficiency using a photomultiplier tube (PMT). The PMT is situated outside the vacuum chamber and fluorescence is coupled to it via a lens inside the chamber. Figure 2 shows the output of the PMT as L3 is scanned across the $3S_{1/2} \rightarrow 10p$ transition, and the two $10p$ fine structure components are clearly resolved.

In order to determine the frequency separation of the fine structure states, we put optical sidebands on L3 at a known frequency spacing. To do this, we modulate the laser current at a frequency f_{sb} and obtain three distinct optical frequencies: f_0, $f_0 \pm f_{\text{sb}}$, where f_0 is the lasing frequency with no modulation and $f_0 \pm f_{\text{sb}}$ are the frequencies of the optical sidebands. For $f_{\text{sb}} < 160$ MHz the laser current is modulated by a PTS160 synthesizer with an accuracy of 0.1 ppm. For $f_{\text{sb}} > 160$ MHz a voltage-controlled oscillator is used. In both cases the frequency is also measured by a frequency counter, Fluke PM6685, with an accuracy of better than 10 ppm. Figure 3 shows the fluorescence detected by the PMT as a function of time when 159.000 MHz sidebands are imprinted on L3 and the laser frequency is scanned across the $3S_{1/2} \rightarrow 10p$ transition. Three distinct pairs of peaks are observed, one for each of the two sideband lasing frequencies and one for the main lasing frequency of L3. The two peaks within each pair are separated by the $10p$ fine structure splitting, and the pairs themselves are separated by the sideband frequency.

The procedure we use to determine the fine structure interval is to scan the L3 optical frequency (with sidebands
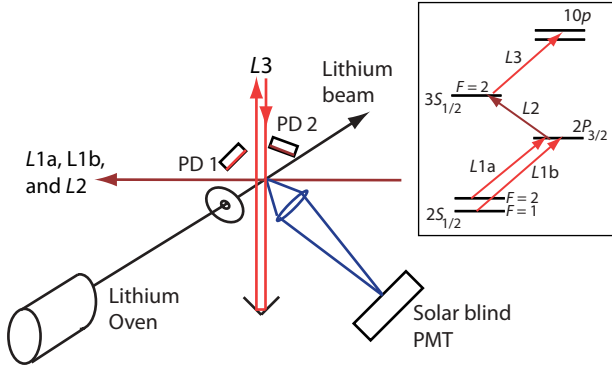
FIG. 1. (Color online) Apparatus used to laser excite ^{7}Li to the $10p$ atomic state via the $2P_{3/2}$ and $3S_{1/2}$ states. Photodiodes 1, 2 (PD1, 2) detect fluorescence from the $2P_{3/2}$ and $3S_{1/2}$ states while the PMT detects $10p$ fluorescence to the ground state. Inset shows energy levels involved in the excitation to the $10p$ state.

present) to generate data similar to that shown in Fig. 3. We assume the frequency scan is linear in time and calculate the frequency scan rate, α, given by

$$\alpha = \frac{(w_1 + w_2 + w_3 + w_4)\,f_{\rm sb}}{(w_1\Delta t_1 + w_2\Delta t_2 + w_3\Delta t_3 + w_4\Delta t_4)}. \quad (1)$$

The quantities w_1, w_2, w_3, and w_4 are the statistical weights for the time intervals Δt_1, Δt_2, Δt_3, and Δt_4 (see Fig. 3) found from a six-Gaussian fit to each laser sweep. The $10p$ interval is then given by

$$\Delta f_{10p} = \frac{\alpha}{3}(\Delta t_{10p1} + \Delta t_{10p2} + \Delta t_{10p3}), \quad (2)$$

where the quantities Δt_{10p1}, Δt_{10p2}, and Δt_{10p3} are three measurements of the $10p$ interval, one for each sideband and one for the main lasing frequency. In this way, the sidebands at a known frequency provide a means to calibrate the $L3$ scan and determine the $10p$ fine structure interval. This technique is a variant of the technique used to study the fine and hyperfine structure of Li$^+$ [14].

III. RESULTS AND DISCUSSION

A total of 1,546 scans similar to the one shown in Fig. 3 were taken at eight different sideband frequencies between 139 and 270 MHz. For each scan the fine structure interval is calculated using Eqs. (1) and (2). Scans with the same $f_{\rm sb}$ are grouped together, and the results are shown in Fig. 4. At each sideband frequency, half the data are taken while the $L3$
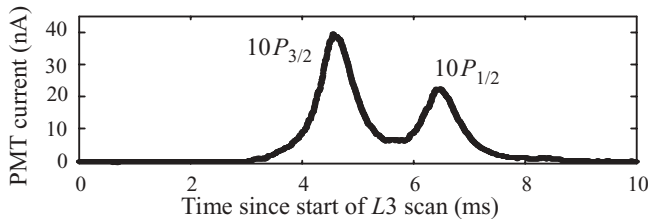

FIG. 2. The $10p \to 2S_{1/2}$ fluorescence detected by the PMT as the $L3$ optical frequency is scanned across the $10p$ resonance. Fluorescence from the two $10p$ fine structure levels are clearly resolved.
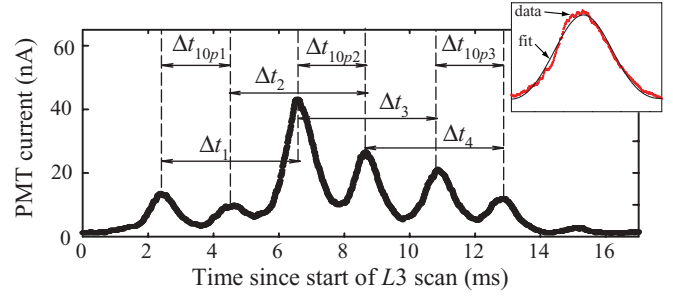

FIG. 3. (Color online) The $10p \to 2S_{1/2}$ fluorescence as $L3$ (with optical sidebands) is scanned across the $10p$ states. Inset shows a slight asymmetry in the fluorescence data when $L3$ is scanned up through the $10p$ states.

optical frequency is being increased, to scan up through the $3S_{1/2} \to 10p$ transition, and half are taken while the frequency is decreased, to scan down through the transition. We combine the results from Fig. 4 and find the fine structure interval to be 74.97 (38) MHz. The uncertainty in parentheses is the standard deviation from the mean, treating measurements at each sideband frequency as independent from one another.

Calculating the fine structure interval using Eqs. (1) and (2) assumes that the $L3$ laser frequency is varying linearly with time. Since the displacement of the PZT is not perfectly linear with applied voltage, even over the small scan ranges used here, the assumption of a linear frequency scan is an approximation. Averaging measurements of the fine structure interval when the laser frequency is scanned up and down is a way to reduce the effect of scan nonlinearity. Table I shows the difference between the intervals measured with $L3$ frequency increasing ($\uparrow$) and decreasing ($\downarrow$), and the difference is statistically significant. Some of this difference is likely due to scan nonlinearity and some is due to a small asymmetry present in the fluorescence peaks recorded while scanning the laser frequency up (see inset of Fig. 3). This asymmetry could be due to the nonlinear scan itself or to some more complex reason. For example, scanning the laser frequency in different directions results in a different $10p$ fine structure component coming into resonance first. If exciting different fine structure components affects the population distribution in the lower atomic levels by an optical pumping effect, it is possible that
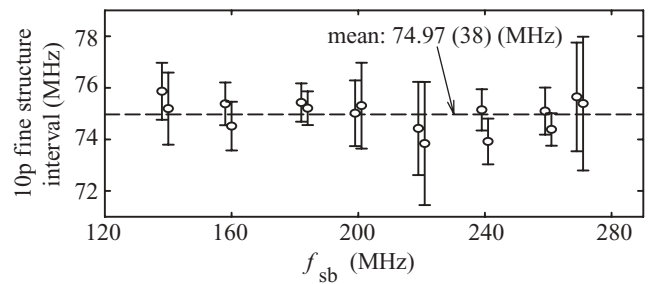

FIG. 4. The $10p$ fine structure interval measured using different sideband frequencies. For each frequency there are two data points: the left-hand one is when the $L3$ optical frequency is scanned up, and the right-hand one is when the optical frequency is scanned down. They are offset horizontally for clarity. The error bars are standard deviations from the mean for all up or down scans at a given $f_{\rm sb}$.

TABLE I. Difference ($\uparrow - \downarrow$) between fine structure intervals measured by scanning $L3$ with its frequency increasing ($\uparrow$) and decreasing ($\downarrow$), at different sideband frequencies. The weighted average difference of all the data is $+0.63$ (0.51) MHz. Numbers in parentheses represent the standard deviation from the mean difference. All units are MHz.

f_{sb}	$\uparrow - \downarrow$
139	0.67 (1.78)
159	0.86 (1.25)
181	0.22 (0.99)
200	-0.29 (2.10)
220	0.58 (2.99)
240	1.22 (1.19)
260	0.71 (1.11)
270	0.26 (3.34)
All	**0.63 (0.51)**

TABLE II. Measured and calculated energy and quantum defect of the $10p$ state.

E_{10p} (cm^{-1})	δ_{10p}	Reference
42379.498 (23)	0.04694 (10)	This work
42379.16 (36)	0.0485 (16)	[11] Experiment
42379.48 (60)	0.047 (3)	[12] Experiment
42379.569	0.04662	[7] R-matrix theory
42379.479	0.04702	[7] Defect function

the fluorescence detected later in the scan would be changed and result in an asymmetric line shape.

To test for scan nonlinearity we compare the time intervals Δt_1, Δt_2, Δt_3, and Δt_4, as defined in Fig. 3. Since these intervals all correspond to exactly f_{sb} we can calculate four separate scan rates (α_1, α_2, α_3, and α_4) distributed throughout the duration of a scan. Any systematic variation in these scan rates would indicate a scan nonlinearity. We note that since our data analysis takes the average of these four rates any scan nonlinearity is already partially accounted for. A typical variation of the rates is seen in Fig. 5(a) and shows no evidence of scan nonlinearity, whereas a small but statistically significant variation is found in six (of the twenty-two) data sets taken. The largest of these variations is shown in Fig. 5(b). The six data sets that show a nonlinear trend are those with the largest sideband frequencies (220–270 MHz), as would be expected since these require the largest frequency sweep.

The effect of a scan nonlinearity is investigated in the following way. We create simulated data sets (with a known fine structure interval) that would result from scans that have a quadratic or cubic deviation from linearity. The amount of nonlinearity is chosen to give variations in α comparable to
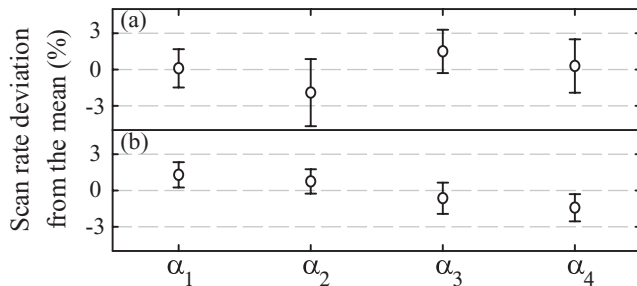
those in Fig. 5. These data sets are analyzed using the same fitting routine we use to analyze the experimental data. From these tests we find that the maximum scan nonlinearity that could be concealed by the scatter and error bars in Fig. 5(a) would shift the $10p$ fine structure interval by ±0.24 MHz, whereas the nonlinearity in Fig. 5(b) would give a -0.14 MHz shift. Since these values are less than the observed differences shown in Table I, we use the observed differences to provide the uncertainty in our measurement due to scan nonlinearity and peak asymmetry. We make a conservative choice for this uncertainty to be the full mean difference (i.e., ±0.63 MHz). Our final result for the $10p$ fine structure interval is then 74.97 (38) (63) MHz, where the first uncertainty is statistical and the second systematic. Combining these uncertainties in quadrature gives a final result for the $10p$ fine structure interval of 74.97 (74) MHz.

Our measurement of the $10p$ interval is more precise by a factor of 5.4 than the best previous measurements of Rydberg p states [4], and we hope it will prompt the calculation of this remaining fine structure interval for the $n = 10$ states. This calculation could be especially interesting since the lithium core plays a significantly larger role for p states than for higher angular momentum states.

Determining the energy of the $10p$ atomic states above the $2S_{1/2}$ ground state, E_{10p}, is straightforward. Our wavemeter reports the wavelength of the $3S_{1/2}$, $F = 2 \rightarrow 10p$ center of gravity to be 659.048(1) nm, where the uncertainty comes from the last reported digit. The wavemeter accuracy is confirmed by measuring the wavelengths of the lithium D_2 lines, which are only 12 nm different from the wavelength of the $3S_{1/2} \rightarrow 10p$ transition and are accurately known [15]. The energy of the center of gravity of the $3S_{1/2}$ state [16] and the $3S_{1/2}$ hyperfine splitting [17] are also accurately known, which allows us to calculate E_{10p} as shown in Table II. Also shown in the table are previous measurements [11,12] and recent theoretical calculations [7] of this energy. To infer the $10p$ energy from [7] we use the precise determination of the ^{7}Li ionization potential (V_I) of 43487.15940 (18) cm^{-1} [8]. The quantum defect of the $10p$ states, δ_{10p}, is given by

$$\delta_{10p} = 10 - \sqrt{109728.73/(V_I - E_{10p})} \qquad (3)$$

and is also included in Table II. It can be seen that our energy and therefore defect measurement agrees very well with the quantum defect function result of Ref. [7] and is close to the R-matrix calculation. Our results are considerably more precise than previous measurements.

FIG. 5. Scan rates measured during different parts of the $L3$ optical frequency scan: (a) shows a typical variation for $f_{sb} =$ 159 MHz, where the scatter and error bars could conceal a nonlinear trend, and (b) shows $f_{sb} = 270$ MHz, where a small systematic scan nonlinearity is seen.

IV. CONCLUSION

We have measured the fine structure interval of the $10p$ atomic state of ^{7}Li with a precision five times greater than previous fine structure measurements of Rydberg ^{7}Li p states.

We hope that this result will stimulate interest in calculating this interval, which has thus far been neglected. We have also measured the energy of the $10p$ state and from this inferred the $10p$ quantum defect, which is in close agreement with recent calculations.

[1] C. Chen, X.-Y. Han, and J.-M. Li, Phys. Rev. A **71**, 042503 (2005).

[2] R. J. Drachman and A. K. Bhatia, Phys. Rev. A **51**, 2926 (1995).

[3] W. E. Cooke, T. F. Gallagher, R. M. Hill, and S. A. Edelstein, Phys. Rev. A **16**, 1141 (1977).

[4] P. Goy, J. Liang, M. Gross, and S. Haroche, Phys. Rev. A **34**, 2889 (1986).

[5] N. E. Rothery, C. H. Storry, and E. A. Hessels, Phys. Rev. A **51**, 2919 (1995).

[6] C. H. Storry, N. E. Rothery, and E. A. Hessels, Phys. Rev. A **55**, 128 (1997).

[7] C. Chao, Commun. Theor. Phys. **50**, 733 (2008).

[8] B. A. Bushaw, W. Nörtershäuser, G. W. F. Drake, and H.-J. Kluge, Phys. Rev. A **75**, 052503 (2007).

[9] M. Anwar-ul-Haq, S. Mahmood, M. Riaz, R. Ali, and M. A. Baig, J. Phys. B **38**, S77 (2005).

[10] L. J. Radziemski, R. Engleman Jr., and J. W. Brault, Phys. Rev. A **52**, 4462 (1995).

[11] R. W. France, Proc. R. Soc. London, Sect. A **129**, 354 (1930).

[12] M. K. Ballard, R. A. Bernheim, and P. Bicchi, Can. J. Phys. **79**, 991 (2001).

[13] G. D. Stevens, C.-H. Iu, T. Bergeman, H. J. Metcalf, I. Seipp, K. T. Taylor, and D. Delande, Phys. Rev. A **53**, 1349 (1996).

[14] J. J. Clarke and W. A. van Wijngaarden, Phys. Rev. A **67**, 012506 (2003).

[15] C. J. Sansonetti, B. Richou, R. E. Engleman Jr., and L. J. Radziemski, Phys. Rev. A **52**, 2682 (1995).

[16] R. Sánchez *et al.*, New J. Phys. **11**, 073016 (2009).

[17] B. A. Bushaw, W. Nortershauser, G. Ewald, A. Dax, and G. W. F. Drake, Phys. Rev. Lett. **91**, 043004 (2003).